Pergamon

Tetrahedron 56 (2000) 6821–6831

TETRAHEDRON

Experimental and Theoretical Host–Guest Photochemistry; Control of Reactivity with Host Variation and Theoretical Treatment With a Stress Shaped Reaction Cavity; Mechanistic and Exploratory Organic Photochemistry[1,2]

Howard E. Zimmerman,* Igor V. Alabugin and Valeriya N. Smolenskaya

Contribution from the Chemistry Department of the University of Wisconsin, Madison, WI 53706, USA

Received 24 July 1999; accepted 7 September 1999

Abstract—In our previous studies prediction of the course of photochemical reactions in crystalline media was accomplished using molecular mechanics with imbedded quantum mechanically generated transition structures. However, there was a need for subsequent geometry optimization of the transition structure within the surrounding 'mini-crystal lattice'. One new approach was devised in which the molecules surrounding the transition structure were replaced by a rigid shell of inert gas atoms with subsequent ab initio geometry optimization of the imbedded transition structure. The present study aimed at providing a more realistic environment surrounding the reacting species. This made use of the recently developed Oniom computations of GAUSSIAN98 which permit ab initio computations on the reacting species while performing molecular mechanical computations on the surrounding molecules. Included was determination of the effect of reaction cavity size. A new analysis, 'Pairs', was developed giving the specific important interactions of atom pairs in a large system. Additionally, the present study extended our solid-state photochemistry to inclusion compounds. This study was both experimental and theoretical. Experimentally, five host–guest inclusion compounds having 4-*p*-cyanophenyl-4-phenylcyclohexenone as the guest were prepared and studied. Three afforded photoproduct resulting from cyanophenyl migration paralleling the regiochemistry in solution; however, the minor products of the solution chemistry were lacking. Strikingly, a fourth inclusion compound gave mainly phenyl migration. The fifth inclusion compound led to 1:1 phenyl versus cyanophenyl migration. The chiral hosts permitted synthesis of enantiomerically pure photoproducts. The Oniom computations required modification but properly predicted migratory behavior in accord with the experimental observations. Several theoretical conclusions in the present study were: (a) the effect of cavity size; (b) the role of crystal relaxation and long range stress effects; (c) the reliability of least motion in predicting reactivity.

Introduction

Much of organic photochemistry has focused on solution reactivity. However, solid-state photochemistry is interesting for a number of reasons. First, the course of the reaction often differs from that in solution and reactions not possible in solution may be obtained. Secondly, the factors controlling the course of the solid-state reactions still are uncertain. Our interest in solid-state chemistry goes back more than a decade. In these previous studies in solid-state organic photochemistry, we have correlated our experimental results with theory based on a quantitative model with the reacting species surrounded by its neighbors. We termed this aggregate a 'mini-crystal-lattice', this based on X-ray data. Initially we used three properties of the intermediate reacting species, overlap with the surrounding lattice, least motion, and volume increase.[3] In subsequent research[4,5] we used molecular mechanics to assess the energy of a transition structure imbedded in the center of a rigid mini-crystal-lattice. The lattice geometry was obtained from X-ray data and the transition structures utilized were approximated by the first intermediates leading to alternative reaction products. These intermediates were generated by both molecular and quantum mechanics. However, due to the size of the mini-crystal-lattice, it was not possible to quantum mechanically geometry optimize the entire system. Molecular mechanics optimization is unsuitable for open shell species such as triplets. Accordingly, we developed a method[6] wherein the atoms nearest the reacting species were transformed into rigid inert gas atoms and the remaining atoms of the mini-crystal-lattice were annihilated. This approach thus generated a fixed shell with the shape of the original surrounding lattice. With a surrounding rigid inert gas shell, the reacting species was then geometry optimized using ab initio quantum mechanics. However, while solving the problem of proper ab initio geometry optimization of open shell species (e.g. triplets) within the host shell, this approach had the weakness of using an artificial lattice.[7] By including only van der Waals interactions between the reacting species and the host lattice, hydrogen bonding and $\pi-\pi$ effects were omitted.

Keywords: mini-crystal lattice; chiral; host–guest photochemistry.

* Corresponding author. E-mail: zimmerman@chem.wisc.edu

0040–4020/00/$ - see front matter
PII: S0040-4020(00)00504-4

Table 1.

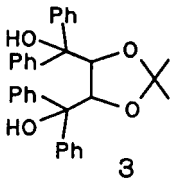

3

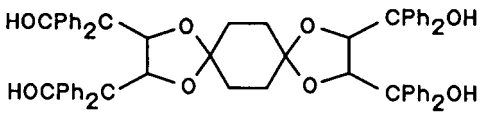

4

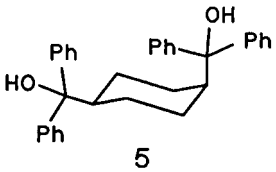

5

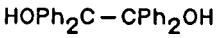

6

Inclusion compound	Enantiomer imbedded	Host:guest ratio	Space group
Seebach–Toda 3	*R*	1:1	$P2_12_12_1$
Seebach–Toda 3	*S*	2:1	$P2_12_12_1$
Octa–Ph–Tetraol 4	*S*	1:1	–
Cy–Hex 5	*RS*	1:1	$P2_1/c$
Benzopinacol 6	*RS*	1:1	*Pbca*

Thus, we needed an approach which would permit ab initio optimization of the guest reacting species while still retaining at least molecular mechanical computation of the entire mini-crystal lattice and also include lattice–guest interaction energy. Recently, Morokuma has devised combined QM/MM methodology incorporated in GAUSSIAN98,[8] and we planned to utilize this approach.

Experimentally, it was our intention to pursue the behavior of reacting species in inclusion compounds; hitherto, our studies have focused on homogeneous crystal lattices. The advantage of host–guest photochemistry is that one can obtain a myriad of different crystal environments, while with simple crystals it is difficult to obtain more than one morphology. The photochemistry of 4-*p*-cyanophenyl-4-phenylcyclohexenone (**1**) as a test case promised to be especially interesting in view of our past studies on the compound, both in solution[9] and in the crystalline state.[10] The solution chemistry is shown in Eq. (1).

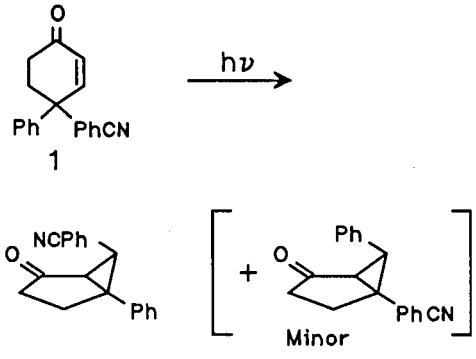

1 (1)

Results: Host–Guest Photochemistry

As noted, different hosts and the corresponding different inclusion compounds can be anticipated to afford different crystal lattices. For the present study four different host molecules were employed. One is the Seebach–Toda compound **3**, also known as Taddol, which has proved useful in forming inclusion compounds.[11] A second was the octaphenyl-tetraol **4**; this followed the philosophy of the Seebach–Toda structure but designed to be larger and more extended. The synthesis simply involved the reaction of diethyl D- or L-tartrate with 1,4-cyclohexanedione followed by reaction with phenylmagnesium bromide. A third host, *cis*-1,4-di(diphenyl-hydroxymethyl)cyclohexane **5**, was synthesized and proved especially useful. A last host used was benzopinacol **6**.

The Seebach–Toda host gave two different inclusion compounds. One was a 1:1 complex **3Ia** while the other was a 2:1 (host:guest) **3Ib**. In the crystallizations using the Seebach–Toda host two observations were made. (a) The 1:1 and 2:1 inclusion complexes (i.e. **3Ia** and **3Ib**) contained different enantiomers. (b) Finally, recovered unincluded enone was found to be essentially enantiomerically pure. The enantiomers selectively complexed in the different chiral hosts are outlined in Table 1.

Partially in analogy, Octa–Ph–Tetraol **4** selectively included the *S*-enantiomer; and the unincorporated enone, again, was one enantiomer, the *R* isomer. This 1:1 complex **4I** contained two molecules of ether in addition to the enone. A cogent point is that in addition to the photochemical usages of the chiral inclusion compounds, these are useful for resolution. Thus, as noted, one enantiomer is not incorporated into the complex and is available. But, the inclusion compound is a source of the enantiomer generally used photochemically.[12]

The remaining hosts were achiral. Both the cyclohexyl-bis-benzhydrol **5** and benzopinacol **6** afforded 1:1 inclusion compounds, **5I** and **6I**, respectively, in quantitative yields; there was no complication arising from only one of two enantiomers being incorporated.

With five inclusion compounds in hand, we obtained X-ray structures from four of these—the Seebach–Toda 1:1 (**3Ia**),

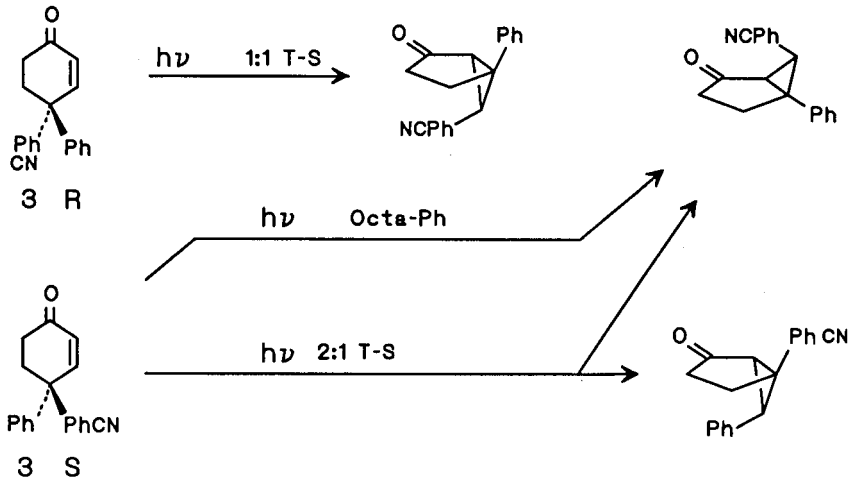

Scheme 1. Regiochemical results of photolysis of the chiral inclusion complexes. Note: T–S refers to the Seebach–Toda Complex **3I** and Octa–Ph refers to the Octa–Ph–Tetraol Complex **4I**.

Seebach–Toda 2:1 (**3Ib**), the Cy–Hex (**5I**) 1:1, and the benzopinacol 1:1 (**6I**) complexes. Next, we proceeded with the irradiation of each of these. In contrast to the solution behavior with preferential cyanophenyl migration, the reaction regiochemistry in the five inclusion compounds was a function of the host structure and the composition of the inclusion compounds.

In the case of the inclusion compound **5I** derived from the cyanophenyl enone **1** and the cyclohexyl-bis-benzhydrol **5**, phenyl migration was preferred 5:1. This, of course, is the reverse of the behavior seen in solution photochemistry. In the case of the Seebach–Toda 2:1 complex **3Ib**, a 1:1 ratio of phenyl to cyanophenyl migration was encountered.

The remaining inclusion compounds—the 1:1 complexes derived from the Seebach–Toda host **3**, the octaphenyl-tetraol **4** host, and from benzopinacol—led to exclusive *p*-cyanophenyl migration. The photolyses of the chiral inclusion compounds are outlined in Scheme 1. The achiral cases gave racemates and their photolyses are depicted in Scheme 2. The mechanistic source of the different reaction regiochemistries is considered in the Interpretative Discussion section.

Another item of interest came from the X-ray analyses of the reactants. In only one case the group which migrated preferentially was equatorial. This differed from our earlier examples.[4] Note discussion below.

Finally, we note that in these irradiations, the photochemistry focussed on conversions below ten percent although rather high conversions were possible without change in the chemistry for several cases. For example, in the case of the benzopinacol complex conversions up to seventy percent led to unchanged regiochemistry. With the inclusion complex **5I** with cyclohexyl-bis-benzhydrol **5** the ratio of phenyl migration diminished. Details on conversions are given in Experimental Section.

Results: Theoretical and Computational Treatment of the Reactions

Recently, very convenient combined quantum mechanics-molecular mechanics programming has become available.[8] This permits ab initio computation on part of a very large molecule while utilizing molecular mechanics on the remainder. This is the method of Morokuma[8a,b] and termed 'Oniom'.[13] Several force fields are incorporated in Oniom. Dreiding[14] and UFF[15] are capable of treating cyano compounds. But, the latter did not have parameterization for hydrogen bonding which is ignored and neither method

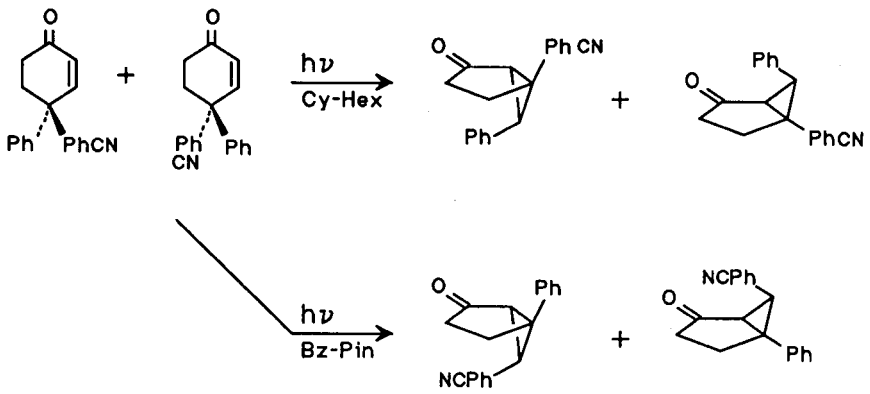

Scheme 2. Regiochemical results of photolysis of the achiral inclusion complexes. Note: Cy–Hex refers to the cyclohexyl-bis-benzhydrol complex **5I** and Bz–Pin refers to the benzopinacol complex.

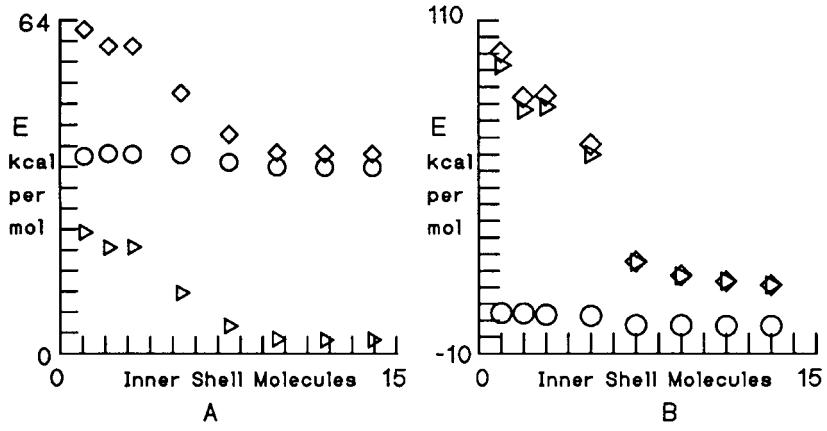

Figure 1. Energies as a function of number of inner shell molecules. diamonds for phenyl, circles for cyanophenyl migration and triangles give the energy difference for the two migrations: A, MM3 values; B, Ab initio energy of the guest.

gave consistent results with the type molecules typical of our organic photochemistry. Additionally, our total number of atoms was beyond that handled by ONIOM, circa 4000. In this computation, three layers were included: (a) the reactant molecule; (b) an inner shell of molecules surrounding the reactant; and (c) an outer shell surrounding the inner shell.

We used MM3[16] pre-optimization of the reacting guest and a next (inner) shell of circa 800 surrounding molecules, keeping the outer shell frozen. The inner shell was taken such that increasing their number did not change the total MM3 energy. (e.g. See Fig. 1). Addition of further layers to the outer shell also did not affect the guest energy or geometry of the included guest molecule. With this approach ONIOM now needed to deal only with the reactant guest molecule and the inner shell, since the inner shell already had been optimized within the rigid outer shell by MM3; and the 4000 atom limitation was circumvented. A major effect of the pre-optimization is to relax the inner lattice shell surrounding the central, reacting guest and thus 'soften' the reaction medium. Any change in the geometry of reacting guest by the pre-optimization is unimportant since this is followed by the ONIOM ab initio geometry optimization. In addition to providing a reasonable lattice, this approach gave information on the role of distant molecular stress effects (vide infra). Finally, following the pre-optimization, Oniom optimization was carried out on the

Table 2. Energies of alternative intermediates for the inclusion compounds

Inclusion compound	Ph migration intermediate[a]	CN–Ph migration intermediate[a]	ΔE[b]	Type of computation[c]
Seebach–Toda 1:1	−851.4088	−851.4272	11.5	ONIOM(3-21G)/Dreiding MM
3Ia	−850.6172	−850.6317	9.1	ONIOM(3-21G)/MM3 Substitution
	−855.4092	**−855.4249**	**9.9**	**ONIOM(6-31G*)/MM3 Substitution**
	1.5988	1.5861	8.0	Dreiding MM
	2.0984	2.0841	8.9	MM3
	−857.4235	−857.4230	−0.3	ROHF/6-31G*, isolated biradical
Seebach–Toda 2:1	−851.1435	−851.1285	−9.4	ONIOM(3-21G)/Dreiding MM
3Ib	−850.1239	−850.1292	3.3	ONIOM(3-21G)/MM3 Substitution
	−854.9183	**−854.9208**	**1.6**	**ONIOM(6-31G*)/MM3 Substitution**
	1.8659	1.8853	−12.2	Dreiding MM
	2.5912	2.5895	1.1	MM3
	−857.4193	−857.4298	6.6	ROHF/6-31G*, isolated biradical
Cyclohexyldiol	−851.2798	851.3080	17.7	ONIOM(3-21G)/Dreiding
5I	−850.7607	−850.7607	0.0	ONIOM(3-21G)/MM3 Substitution
	−855.5556	**−855.5523**	**−2.1**	**ONIOM(6-31G*)/MM3 Substitution**
	1.7268	1.7095	10.9	Dreiding MM
	1.9535	1.9581	−2.9	MM3
	−857.4189	−857.4294	6.6	ROHF/6-31G*, isolated biradical
Benzopinacol	−851.4613	−851.4659	2.9	ONIOM(3-21G)/Dreiding
6I	−850.4788	−850.4986	12.5	ONIOM(3-21G)/MM3 Substitution
	−855.2728	**−855.2893**	**10.4**	**ONIOM(6-31G*)/MM3 Substitution**
	1.5470	1.5530	−3.8	Dreiding MM
	2.2351	2.2207	9.0	MM3
	−857.4181	−857.4284	6.5	ROHF/6-31G*, isolated biradical

[a] Absolute energies are in Hartrees (627.5 kcal mol^{-1}).
[b] Energy differences are in kcal mol^{-1}.
[c] Six methods, each for Oniom (Rohf/3-21G)/Dreiding geometry but subsequent computation as indicated, (i) Original computation, (ii) Substitution of MM3 for Dreiding energies, (iii) Same as (ii) but with 6-31G*, (iv) Dreiding MM on entirety, (v) MM3 on entirety, (vi) ROHF on the central, triplet guest alone as optimized within the shell. The bold lines contain the preferred computation.

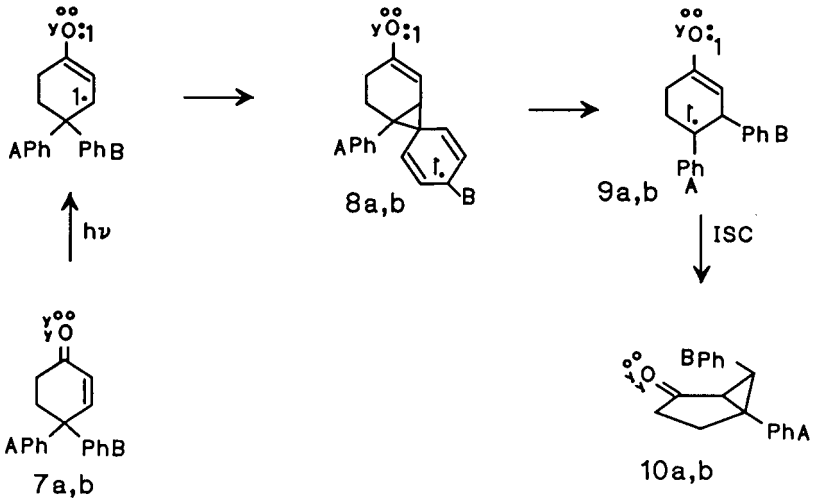

Scheme 3. Type B enone rearrangement mechanism. Note: **8a** A=H, B=CN for Cyanophenyl Migration; **8b** A=CN, B=H for phenyl migration. The three-dimensional $n-\pi^*$ configuration is shown with y's as in-plane p_y electrons, solid dots as π-system electrons, and small circles as sp-hybrid electrons.[17]

central lattice system (guest+inner shell) with the outer lattice shell being held fixed.

We note that Oniom affords its energies in three components which comprise the total; note Eq. (2). Thus there is flexibility in taking an Oniom computation and replacing one or more of the three ONIOM components obtained. This, in effect, is an improvement of the original Oniom results with the molecular mechanics components being replaced by their MM3 counterparts (note computation details below).

$$E_{tot} = E_{inner}(\text{ab initio}) + E_{outer}(\text{MM}) - E_{inner}(\text{MM}) \qquad (2)$$

Table 2 gives energies for the phenyl and cyanophenyl migration intermediates (**8a** and **8b**, note also Scheme 3) and compares the two alternative reaction routes. For each route, six entries corresponding to different theoretical treatments are given. Thus, the first treatment of the six corresponds to utilization of Oniom computations without modification. The second entry has the calculated MM3 energy replacing the Dreiding component. The third entry differs only in a 6-31G* basis replacing the 3-21G of the previous line. The fourth and fifth items compare Dreiding and MM3 molecular mechanics computations for the entire lattice without use of quantum mechanics. The last entry gives the ROHF/6-31G* energy of the triplet reaction intermediate with geometry optimized within the shell. The ΔE's given correspond to the difference in energies between the phenyl migration and cyanophenyl migration species in the medium specified. A negative ΔE corresponds to preferential phenyl migration while a positive value would predict cyanophenyl bridging. As is discussed in the Interpretative Discussion Section (vide infra), although several computational methods correctly predict experiment for one or more of the four inclusion complexes, only entry three ONIOM (6-31G*)/MM3 fits all four cases.

Table 3. Energies of alternative migrating species without pre-optimization

Inclusion compound	$\Delta E^{a,b}$	Inclusion compound	$\Delta E^{a,b}$
Seebach–Toda 1:1 3Ia	−1.4	Cyclohexyldiol 5I	14.7
Seebach–Toda 2:1 3Ib	7.0	Benzopinacol 6I	35.8

[a] Computations using the ab initio/6-31G* with MM3 replacement of Dreiding energies but without pre-optimization.
[b] kcal mol^{-1}.

It is of interest to consider the importance of the MM3 pre-optimization used in these computations. Table 3 gives the ΔE values for Oniom/(6-31G*)/MM3 without pre-optimization. A more complete table is given in Appendix A. We note that preferential phenyl migration in inclusion compound **5I** is never predicted without this use of MM3.

Interpretative Discussion

In the rearrangement of 4-cyanophenyl-4-phenylcyclohexenone the preferential cyanophenyl migration has been noted[9] to arise from the greater delocalization resulting when the cyano substituent in intermediate **8** (see Scheme 3) is on the migrating group. The reasoning agrees with the experimental observation[18] that cyano substitution on the migrating group has a large positive rate effect while there is a minimal acceleration with substitution on the non-migrating; this demonstrates that the rate-limiting portion on the hypersurface comes early and involves the migration. This reasoning has now been confirmed by ab initio computations at the ROHF/6-31G* level which indicate that the lowest energy triplet bridged species has cyanophenyl migrating. A minor complication is that, for each migrating group, there are two local minima, differing in the dihedral angles of the $-CH_2-CH_2$ group. These derive computationally, using least motion, from equatorial and axial groups migrating. However, for each conformation, cyanophenyl migration is preferred as noted in Table 4.

Table 4. Gas phase energies of the bridged triplet species **8**

Structure of intermediate	E (ROHF/6-31G*)	ΔE (kcal mol^{-1}
8a (Equatorial PhCN)	−857.4331	0
8b (Equatorial Ph)	−857.4280	3.2
8a (Axial PhCN)	−857.4292	2.5
8b (Axial Ph)	−857.4241	5.7

Table 5. RMS motion values (RMS values are in Å)

Inclusion	Migrating group	RMS motion	Inclusion complex	Migrating group	RMS motion
Seebach–Toda **3Ia**	Phenyl	0.94	Cy–Hex **5I**	Phenyl	1.52
Seebach–Toda **3Ia**	Cyano–Ph	1.23	Cy–Hex **5I**	Cyano–Ph	0.97
Seebach–Toda **3Ib**	Phenyl	1.39	Benzopin **6I**	Phenyl	1.58
Seebach–Toda **3Ib**	Cyano–Ph	0.80	Benzopin **6I**	Cyano–Ph	0.82

Some explanation of Table 4 is needed. Thus, there are two conformers of the enone reactant, one with the cyanophenyl pseudo equatorial and the other with this group pseudo axial. In our previous studies we have found that often it is the pseudo equatorial group which migrates preferentially. Not only is the ipso carbon of an equatorial aryl group marginally closer to the enone β-carbon (circa by 0.1 Å from AM1 geometry), but more importantly the preferred conformation is found to have the π-system of the equatorial aryl group facing the enone β-carbon while the edge of the axial aryl tends to be oriented towards the β-carbon. This is observed both for isolated molecules and in most enone crystal lattices we have studied.[4]

In solution one often has a myriad of potential conformations of a reacting species to consider. In contrast, for each inclusion compound there will be a specific frozen geometry. Of the four inclusion compounds presently studied one, the Seebach–Toda 1:1 complex **3Ia**, had the cyanophenyl group pseudo axial. The remaining three-the Seebach–Toda 2:1 complex **3Ib**, the benzopinacol **6I** complex, and the Cy–Hex **5I**-all possessed pseudo equatorial cyanophenyl groups. Hence, one unique facet of crystal lattice photochemistry is that one is dealing with reactivity of isolated frozen conformers, here each with an axial or an equatorial arrangement. Nevertheless, the axial versus equatorial relationship did not directly correlate with the regioselectivity of migration in the present study.

Thus, the Cy–Hex inclusion complex **5I**, which had a pseudo equatorial cyanophenyl group exhibited mainly axial phenyl migration. The Seebach–Toda 2:1 complex **3Ib** which also had a pseudo equatorial cyanophenyl group led to 1:1 axial phenyl and equatorial cyanophenyl migration while the benzopinacol complex with a similar conformation gave only equatorial cyanophenyl migration. Finally, the Seebach–Toda 1:1 complex **3Ia** which had an axial cyanophenyl group exhibited axial cyanophenyl migration.

The most striking result is the preferential phenyl migration in the Cy–Hex complex **5I**. The 1:1 regioselectivity of the Seebach–Toda 2:1 complex **3Ib** is also rather interesting. We see that the electronic factor favoring cyanophenyl migration is overridden by the necessity of reacting in an irregular cavity. Overall, there is an extreme variation of regioselectivity with a total dependence on the specific host employed.

It was especially interesting to find that in the crystal lattice photochemistry, not only did the migratory behavior depend on the host and the crystal lattice, but also that the crystal lattice forces could override the gas phase electronic effect with the result of predominant phenyl migration in one case. This then further illustrates the control of excited state transformations by the shape of surrounding crystal lattices. Thus, a reaction less favored in solution or the gas phase by an energy of at least 3.2 kcal mol^{-1} (see Table 4) can be obtained in the solid state.

A final aspect deals with the concept of least motion. Least motion needs to be thought about in terms of the required motion in proceeding from the actual reactant geometry in the inclusion compound to afford the bridged triplet diradicals **8a** and **8b**. This principle is violated in three of the four cases presently studied. The RMS Motion Values obtained from Macromodel[19] are given in Table 5. In agreement with the qualitative discussion less motion is required. In fact, in some of our previous studies[4] there was a preference for migration of the equatorial group in accord with least motion effects. More recently least motion was found to be unreliable[5] and the present study confirms that unreliability.

Having discussed least motion as not being controlling, we now need to discuss what is controlling. One clue comes from the 'Pairs Analysis' which determines which atom pairs are closest and contribute most to the stabilization or destabilization of the host–rearranging triplet inclusion complex. One observation from the pairs analysis is that the preferred intermediate species invariably has a close hydrogen bonding interaction between a host hydroxyl and the triplet oxygen; these are stabilizing interactions. But additionally, the preferred intermediates imbedded in the relaxed lattice, but not in the frozen one, lack the close repulsive atom–atom proximities seen for the unfavored species.

Another item requiring discussion is the relaxation of the inner shell of molecules immediately surrounding the reacting guest. In the present study, this role was played by the pre-optimization. Thus, pre-optimization permits the inner-shell to relax and takes lattice stress into account. Not only shape but also the mechanical properties of the lattice are included since the cavity becomes adaptable to the guest.

Closely related and of real interest is the evidence bearing on long range stress effects. This comes from Fig. 1 which gives the total energy as a function of number of molecules considered as inner shell entities. Remembering that the inner shell molecules are subject to relaxation in the pre-optimization, we note that with a relatively small number of inner shell molecules, the energy diminishes as we increase the number of molecules subject to relaxation. However, a limit is rapidly reached and addition of further molecules which may relax does not lower the total energy further. This provides a good assessment of distance at which stress effects are relevant. This distance is in the range of 20 to 30 Å and this corresponds to one layer of neighbors surrounding the reacting species. This result accords with

the suggestions of McBride[20] regarding the role of crystal stress on the reaction course.

Conclusion

This study has presented new host–guest photochemistry and has focussed on the use of ONIOM computations to permit ab initio geometry optimization of open shell species. It has dealt with the role of crystal lattice relaxation, stress effects and cavity dominance over electronic effects.

Over the last decade our aim in solid-state photochemistry has been to determine what factors are controlling. A wealth of superb literature efforts have had the same pursuit.[21] We note that about a decade ago Gavezzotti commented[21a] that 'The general problem of obtaining information on solid-state reactivity from a theoretical calculation has not yet been tackled in a systematic way'.[21a] Nevertheless, over this last decade there has been a variety of approaches,[21] many elegant.

Experimental

General procedures

All reactions were performed under an atmosphere of dry nitrogen. Column chromatography was performed on silica gel (Matheson, Coleman and Bell, grade 62, 60–200 mesh) mixed with Sylvania 2282 phosphor and slurry packed into quartz columns to allow monitoring with a hand-held UV lamp. Melting points are uncorrected. ^{1}H and ^{13}C NMR spectra were recorded at 300 and 75 MHz respectively, using $CDCl_3$ as solvent and are reported in ppm downfield from tetramethylsilane. Solvents were dried following standard methods.

General procedure for X-ray crystallography analysis

X-Ray diffraction data were collected on a Siemens P4/CCD diffractometer for single crystals of each compound. Lorentz and polarization corrections were applied and each structure was solved under the appropriate space group symmetry by direct methods using SHELX86 or SHELXTL.[22] Hydrogen atom positions were calculated and refined with a rigid model. Full-matrix least-square refinement on F^2 was carried out employing anisotropic displacement parameters for all non-hydrogen atoms and isotropic displacement parameters for all hydrogen atoms. The coordinates for all compounds studied by X-ray crystallography were deposited with the Cambridge Crystallographic Data Center. The coordinates can be obtained, on request, from the Director, Cambridge Crystallographic Data Center, 12 Union Road, Cambridge, CB2 1EZ, UK.

General procedure for solid-state photolysis

Large crystals were gently cracked and placed between two Pyrex slides. The slides were placed in a Pyrex beaker filled with water and placed in a larger beaker filled with mixture of ice and water. The slides were 2.5 cm from a 400 W Mercury lamp with a water cooling well. The samples were photolyzed through a 2-mm Pyrex filter. The reaction mixtures were dissolved in $CDCl_3$ after photolysis, dried over sodium sulfate, analyzed by ^{1}H NMR and separated by column chromatography on silica gel.

(*R*,*R*,*R*,*R*)-Tetraethyl-1,4,9,12-tetraoxadispiro[4.2.4.2]-tetradecane-2,3,10,11-tetracarboxylate. A solution of 2.24 g (20 mmol) of 1,4-cyclohexanedione, 8.6 g (40.5 mmol) of the diethyl ester of (*R*,*R*)-tartaric acid and 0.40 g of *p*-toluenesulfonic acid in benzene was refluxed with azeotropic removal of water for 30 h. The cooled reaction mixture was washed with saturated sodium bicarbonate, then water, extracted with methylene chloride and dried over magnesium sulfate. Removal of solvent in vacuo afforded 9.4 g (96%) of oily product which was pure by NMR analysis and could be directly used in the next reaction with phenylmagnesium bromide. An analytical sample was obtained by extraction of the oil with boiling heptane to give white thin plates, mp 63–76°C, followed by crystallization from ethanol. White needles, mp 75–77°C. ^{1}H NMR ($CDCl_3$, TMS): δ 4.79 (s, 4H), 4.30–4.23 (q, 8H, J=6.9 Hz), 1.95 (s, 8H), 1.31 (t, 12H, J=6.9 Hz,). ^{13}C NMR: 169.78, 113.25, 77.0, 61.88, 32.76, 14.07. IR (KBr): 2940, 2978, 1753, 1584, 1221, 1128. $[\alpha]_D^{20}=-27$ (acetone, c2=0.080). HRMS, *m/e* (M^+): 488.4815. Calcd for $C_{22}H_{32}O_{12}$, 488.4823. Anal. Calcd for $C_{22}H_{32}O_{12}$: C, 54.09, H, 6.60. Found: C, 53.85, H, 6.73. The (*S*,*S*,*S*,*S*)-isomer was obtained in a similar manner.

(*R*,*R*,*R*,*R*)-Diphenyl(3,10,11-tri(hydroxy(diphenyl)methyl)-1,4,9,12-tetraoxadispiro[4.2.4.2]tetradec-2-yl)methanol (4). To a solution of 9.0 mmol of phenylmagnesium bromide in 25.0 ml of THF at 0–5°C was added a solution of 488 mg (1.0 mmol) of (*R*,*R*,*R*,*R*)-tetraethyl-1,4,9,12-tetraoxadispiro[4.2.4.2]tetradecane-2,3,10,11-tetracarboxylate in 8.0 ml of THF. The solution was stirred at −5°C for 1 h, warmed to room temperature and refluxed for 9 h. The reaction mixture was poured into 100 ml of saturated ammonium chloride solution and extracted with methylene chloride. The combined organic fractions were washed with water and dried over magnesium sulfate. Solvent was removed in vacuo at 50°C to afford a 1:4 complex of the product and THF as a viscous oil. The oil was dissolved in 80 ml of carbon tetrachloride, concentrated again in vacuo and dried at 8 mm Hg/80°C for 3 h to afford 0.95 g of an yellow solid. The solid was dissolved in hot methanol, refluxed for 5 min and cooled to −5°C. White crystals of complex with methanol were filtered, mp 273°C. The guest-free host was obtained by removal of the guest solvent in vacuo. The yield was 0.69 g (74%) of white solid, mp 269–271°C. ^{1}H NMR ($CDCl_3$, 300 MHz): δ 7.3 (m, 40H), 4.6 (s, 4H), 4.0 (s, 4H), 1.4 (m, 8H). ^{13}C NMR: 145.86, 142.43, 128.50, 128.18, 127.56, 127.18, 109.15, 80.40, 78.15, 33.37. IR (KBr): 3389, 3089, 3058, 3033, 2961, 2924, 1635, 1494, 1447, 1376, 1139, 1100. $[\alpha]_D^{20}=-19$ (acetone, c=0.054). HRMS, *m/e* (M^+): 929.1041. Calcd for $C_{62}H_{56}O_8$, 929.1032. Anal. Calcd for $C_{62}H_{56}O_8$: C, 80.15, H, 6.08. Found: C, 79.98, H, 6.19. This structure was confirmed by X-ray analysis of complex with CH_2Cl_2. The (*S*,*S*,*S*,*S*)-isomer was obtained in a similar manner.

***cis*-1,4-Di(diphenylhydroxymethyl)cyclohexane (5).** A

solution of 7.0 g (0.035 mol) of dimethyl 1,4-cyclohexanedicarboxylate (a 1.7:1 mixture of *cis*- and *trans*-isomers) in 45 ml of THF was added to a solution of 5 equivalents of phenylmagnesium bromide in 50 ml of THF at room temperature. The reaction mixture was refluxed for 13 h, then poured into 100 ml of saturated NH_4Cl solution and chloroform extracted. The combined organic fractions were washed with water, dried over magnesium sulfate, and concentrated in vacuo to afford 12.3 g (78.5%) of white crystals of a mixture of *cis*- and *trans*-isomeric products. The *cis*-isomer, 2.6 g (33.6%, based on *cis*-ester), was isolated by fractional crystallization from 7:1 ethanol:chloroform; mp 195–196°C. ^{1}H NMR ($CDCl_3$): δ 7.3 (m, 20H), 2.7 (br.s., 2H), 2.15 (s, 2H), 1.5 (m, 8H). HRMS *m*/*z* (M^+) Calcd for $C_{32}H_{32}O_2$: 448.6101, Obsd: 448.6113. ^{13}C NMR ($CDCl_3$): 146.8, 128.1, 126.3, 125.6, 81.4, 40.4, 23.8. The structure was established by X-ray analysis of the inclusion compound (vide infra).

Crystallization behavior of 4-cyanophenyl-4-phenylcyclohexenone and (*R*,*R*,*R*,*R*2)-'octaphenyltetraol' (4) system. *Using a 1:1 host:guest ratio*. A solution of 186 mg (0.20 mmol) of (*R*,*R*,*R*,*R*)-(**4**) and 55 mg (0.20 mmol) of the enone (**1**) in 15 ml of 1:1 ether:hexane was left covered with 'Parafilm' with several small apertures for one day. The crystals had a 0.55:1 guest:host ratio. The complex contained two equivalents of ether as a third component.

Using 2:1 a host:guest ratio. (a) A solution of 186 mg (0.20 mmmol) of the host (**4**) and 110 mg (0.40 mmol) of the enone (**1**) in 15 ml of 1:1 ether:hexane was left covered with 'Parafilm' with several small apertures. The crystals of the 1:1:2Et_2O complex (240 mg, 91%) were formed overnight. The melting behavior of the complex was interesting. At 138°C, the compound melted and very intensive evaporation of ether was observed. Then the melt solidified again and melted in the range of 230–244°C. (b) A solution of 1.696 g (1.82 mmmol) of the host (**4**) and 998 mg (3.65 mmol) of the enone (**1**) in 40 ml of 1:1 ether:hexane was left covered with 'Parafilm' with several small apertures. When 15 ml of the solvent was left crystals of the 1:1 complex were formed as it was described above (2.420 g, 98 %). After filtration the mother liquor was left covered with 'Parafilm' with several small apertures. White crystals (128 mg, 28.5% on one enantiomer) of the enone were formed overnight, mp 73–76°C, $[\alpha]_D^{20}=+12$ (c=0.10, chloroform).

Using 4:1 a host:guest ratio. A solution of 186 mg (0.20 mmol) of the host (**4**) and 220 mg (0.80 mmol) of the enone (**1**) in 15 ml of 1:1 ether:hexane was prepared. After 15 min, shiny crystals of the inclusion complex formed. In several hours the precipitation was completed to give 238 mg (98%) of fine transparent crystals of the 1:1 complex.

Resolution of racemic 4-cyanophenyl-4-phenylcyclohexenone; enantioselectivity of the inclusion process. *Analysis of the guest inside the inclusion complex*. Refluxing of 270 mg of the complex (**4I**) in methanol resulted in a relatively slow decomposition of the starting inclusion compound and formation of a new complex with methanol. The 4-cyanophenyl-4-phenyl-cyclohexenone remained in solution (48 mg, 88%). $[\alpha]_D^{20}=-11$ (chloroform, c=0.06).

Analysis of the guest left in mother liquor. A solution of 186 mg (0.20 mmol) of the host (**4**) and 110 mg (0.40 mmol) of the enone (**1**) in 15 ml of 1:1 ether:hexane mixture was left covered with 'Parafilm' with several small apertures. The crystals of the 1:1:2Et_2O complex (240 mg, 98%) were filtered. Guest left in the mother liquor (chloroform, c=0.034) had $[\alpha]_D^{20}=+2.5$. Two crystallizations raised the rotation to +13 (chloroform, c=0.028).

Crystallization behavior of 4-cyanophenyl-4-phenylcyclohexenone/'Toda–Seebach' (3) system. *Using a 1:1 host:guest ratio*. A solution of 0.273 g (1.0 mmol) of the enone and 0.466 g (1.0 mmol) of (*R*,*R*)-host (**3**) in 35 ml of 1:1 ether:hexane was covered with 'Parafilm' with several small apertures. Three crystalline fractions were obtained. (a) After 3 days 360 mg (97%, based on one enantiomer of the guest) of 4–6 mm prismatic crystals of the 1:1 inclusion compound (**3Ia**) were formed, mp 123–124.5°C. The mother liquor left in an open flask afforded a mixture of (b) small microcrystalline aggregates (40 mg, 29% of the remaining enantiomer of 4-cyanophenyl-4-phenylcyclohexenone (**1**), mp 75°C) and (c) fine needles of the 2:1 complex (**3Ib**), mp 150–153°C, (170 mg, 28% based on the remaining enantiomer) after standing overnight. Mass-balance 77%, the rest of the reaction mixture was a mixture of small crystals of the enone (**1**) and the 2:1 complex (**3Ib**).

Using a 2:1 host:guest ratio. Solution of 0.506 g (1.853 mmol) of the enone and 0.432 g (0.926 mmol) of (*R*,*R*)-host (**3**) in 40 ml of 1:1 ether:hexane was left covered with 'Parafilm' with several small apertures for 4 days. The solvent volume decreased to 10 ml, and a mixture of large prismatic crystals and small microcrystalline aggregates formed (690 mg). The big prisms were separated by hand (470 mg, 69%) and found to be the 1:1 inclusion compound, mp 123–124.5°C. The microcrystalline aggregates (120 mg, 24%) were found to be 4-cyanophenyl-4-phenylcyclohexenone, mp 75°C, $[\alpha]_D^{20}=-2.6$ (chloroform, c=0.06). The separated mother liquor was left in an open flask and fine needles of the 2:1 host (**3**): enone (**1**) complex were formed after standing overnight (50 mg), mp 151.5–153°C. The mass-balance 68%, the rest of the reaction mixture was a mixture of small crystals.

*Using 2:3 host:guest ratio; the 2/1 inclusion compound (**3Ib**)*. A solution of 0.273 g (1.0 mmol) of the enone and 0.699 g (1.5 mmol) of (*R*,*R*)-(**3**) in 35 ml of 1:1 ether:hexane was kept covered with 'Parafilm' with several small apertures at −20°C. Well-shaped needles of the 2:1 complex (**3Ib**) were formed first, 393 mg, 65% (based on one enantiomer of the guest), mp 151.5–153.5°C. Prisms of the 1:1 inclusion compound crystallized subsequently (**3Ia**), 355 mg, 96% (based on the one enantiomer of the guest), mp 119–122°C. The mass-balance 77%, the rest of the reaction mixture was a mixture of small crystals.

1:1 Complex of *cis*-1,4-di(diphenylhydroxymethyl)cyclohexane and 4-*p*-cyanophenyl-4-phenylcyclohexenone (5I). *cis*-1,4-Di(diphenylhydroxymethyl)cyclohexane 0.10 g

(0.22 mmol) and 0.061 g (0.22 mmol) of the enone were dissolved in 30 ml of 4:1 ether:hexane and left covered with 'Parafilm' with several small apertures. After 2 days crystals of a 1:1 complex were obtained quantitatively; mp 102–105°C. ^{1}H NMR ($CDCl_3$): δ 7.65–7.1 (m, 30H), 6.25 (d, J=7 Hz, 1H), 2.85–2.55 (m, 3H), 2.5–2.25 (m, 2H), 2.15 (s, 2H), 1.75–1.5 (m, 4H), 1.5–1.3 (m, 4H). The structure of the inclusion complex was determined by X-ray analysis.

1:1 Complex of benzopinacol and 4-*p*-cyanophenyl-4-phenylcyclohexenone (6I). Benzopinacol, 0.040 g (0.10 mmol) and 0.030 g (0.10 mmol) of the enone were dissolved in 30 ml of 1:1 ether:hexane mixture and left covered with 'Parafilm' with several small apertures. After 2 days crystals of a 1:1 complex were obtained quantitatively; mp 135–160°C. ^{1}H NMR ($CDCl_3$): δ 7.7–7.15 (m, 30H), 6.25 (d, J=7 Hz, 1H), 3.05 (s, 2H), 2.85–2.6 (m, 2H), 2.5–2.35 (m, 2H). The structure of the inclusion complex was determined by X-ray analysis.

Exploratory solid-state photolysis of the 1:1 complex of 'octaphenyltetraol' (4) and 4-cyanophenyl-4-phenylcyclohex-2-en-1-one. Crystals of the 1:1 complex (**4I**) (120 mg) were photolyzed for 5 h. NMR analysis of the slightly yellow solid reaction mixture indicated formation of *trans*-5-phenyl-6-*p*-cyano-phenylbicyclo[3.1.0]hex-2-one as the only product at a conversion of 26%. The product was isolated by column chromatography on silica gel using 10% ether in hexane as eluent. Fraction 1 contained 6.1 mg (22%) *trans*-5-phenyl-6-*p*-cyano-phenylbicyclo[3.1.0]hex-2-one with all physical and spectral properties identical to the literature data.[9] Fraction 2 contained 19 mg (70%) of the starting material. Fraction 3 contained 88 mg (95%) of the host.

Irradiation under similar conditions of 70 mg of the complex (**4I**) for 8 h afforded only the *trans*-5-phenyl-6-*p*-cyanophenylbicyclo[3.1.0]hex-2-one (conversion 44%, analyzed by ^{1}H NMR).

Irradiation of 70 mg of the complex (**4I**) for 14 h afforded a 4:1 mixture of *trans*-5-phenyl-6-*p*-cyanophenylbicyclo-[3.1.0]hex-2-one and *trans*-5-*p*-cyano-phenyl-6-phenylbicyclo[3.1.0]hex-2-one (conversion 92%, analyzed by ^{1}H NMR).

Exploratory solid-state photolysis of 1:1 complex of 'Toda–Seebach' host (3) and 4-cyanophenyl-4-phenylcyclohex-2-en-1-one. Irradiation of 50 mg of the complex (**3Ia**) under similar conditions for 6 h afforded *trans*-5-phenyl-6-*p*-cyanophenylbicyclo[3.1.0]hex-2-one (conversion 6%, analyzed by ^{1}H NMR).

Irradiation of 50 mg of the complex (**3Ia**) under similar conditions for 12 h afforded *trans*-5-phenyl-6-*p*-cyano-phenylbicyclo[3.1.0]hex-2-one (conversion 19%, analyzed by ^{1}H NMR).

Irradiation of 50 mg of the complex (**3Ia**) under similar conditions for 19 h afforded 3:1 mixture of *trans*-5-phenyl-6-*p*-cyanophenylbicyclo[3.1.0]hex-2-one and *trans*-5-*p*-cyanophenyl-6-phenylbicyclo[3.1.0]hex-2-one (conversion 47%, analyzed by ^{1}H NMR).

Exploratory solid-state photolysis of 2:1 complex of 'Toda–Seebach' host (3) and 4-cyanophenyl-4-phenylcyclohex-2-en-1-one. The 2:1 complex (**3Ib**) (120 mg, 0.10 mmol) was photolyzed for 15 min. NMR analysis of the slightly yellow solid reaction mixture indicated formation of 2:1 mixture of *trans*-5-phenyl-6-*p*-cyanophenylbicyclo[3.1.0]hex-2-one and *trans*-5-*p*-cyano-phenyl-6-phenylbicyclo[3.1.0]hex-2-one (conversion 58%, analyzed by ^{1}H NMR). The products were isolated by column chromatography on silica gel using 10% ether in hexane as eluent. Fraction 1 contained 6.0 mg (22%) of *trans*-5-phenyl-6-*p*-cyanophenylbicyclo[3.1.0]hex-2-one. Fraction 2 contained 3.0 mg (11%) of *trans*-5-*p*-cyanophenyl-6-phenylbicyclo[3.1.0]hex-2-one with all physical and spectral properties identical to the literature data.[9] Fraction 3 contained 9.5 mg (35%) of the starting enone. Fraction 4 contained 84 mg (90%) of the host.

Irradiation of 70 mg of the complex (**3Ib**) under similar conditions for 5 min afforded a 1.2:1 mixture of *trans*-5-phenyl-6-*p*-cyanophenylbicyclo[3.1.0]hex-2-one and *trans*-5-*p*-cyanophenyl-6-phenylbicyclo[3.1.0]hex-2-one (conversion 16%, analyzed by ^{1}H NMR).

Irradiation of 70 mg of the complex (**3Ib**) for 3 min afforded 1.2:1 mixture of *trans*-5-phenyl-6-*p*-cyanophenylbicyclo-[3.1.0]hex-2-one and *trans*-5-*p*-cyanophenyl-6-phenylbicyclo-[3.1.0]hex-2-one (conversion 3 or 7% in two separate runs, analyzed by ^{1}H NMR).

Irradiation of 70 mg of the complex (**3Ib**) for 25 min afforded 2:1 mixture of *trans*-5-phenyl-6-*p*-cyanophenylbicyclo[3.1.0]hex-2-one and *trans*-5-*p*-cyanophenyl-6-phenylbicyclo-[3.1.0]hex-2-one (conversion >77%, analyzed by ^{1}H NMR). Small amount of unindentified products, presumably the result of secondary photochemical products, were also detected by NMR at this conversion.

Photolysis of the inclusion complex (5I). In typical runs, 0.10 g (0.10 mmol) of the crystalline inclusion compound (**5I**) was irradiated between glass slides or in a Pyrex tube (3 mm in diameter) for different periods of time, ranging from 5 to 200 min at 15–18°C. The ratios of the photoproducts obtained by NMR analysis are given in the Table 6.

The NMR data of the three photoproducts corresponded to the known isomeric bicyclic photoketones from photolysis of 4-*p*-cyano-4-phenylcyclohexenone in solution[9] without extraneous peaks from by-products.

Photolysis of the benzopinacol inclusion complex (6I). Crystals of the inclusion complex (**6I**) were irradiated using portions of 0.050–0.070 g. In the NMR spectra the singlet of the benzopinacol hydroxyl groups overlaps with

Table 6.

Time (min)	Conversion (%)	*trans*–Ph/ *trans-p*-CN–Ph	*trans*–Ph/ *cis*–Ph
75	<10	5/1	13/2
135	16	3/1	6/1
200	26	3/2	3/1

the doublets of the bridgehead protons in the photoproducts; thus, the NMR analyses were carried out in the presence of a 0.05 ml of deuterated water for the proton exchange. The exclusive formation of *trans*-5-*p*-cyano-phenyl-6-phenyl-bicyclo[3.1.0]hexan-2-one has been observed at all conversions.

Acknowledgements

Support of this research by the National Science Foundation is gratefully acknowledged with special appreciation for its support of basic research. Also, we wish to acknowledge helpful discussions with, and advice from, Dr Douglas Powell regarding X-ray diffractometry. We are also pleased to acknowledge Departmental NSF grants CHE-9310428 and CHE-9709005 supporting X-ray facilities and NSF CHE-9208463, NIH 1 510 RR0 8391-01 supporting NMR.

Appendix A. Supplementary Material

Analysis results without pre-optimization of the inner shell lattice (no preoptimization of the crystal cavity)

See Tables A1 and A2.

Table A1. MM3 optimizations of the triplet intermediates inside rigid crystal lattices

Inclusion compound	ΔE (Ph–CN–Ph), kcal mol^{-1}
Seebach–Toda 1:1 (**3Ia**)	−12.9
Seebach–Toda 2:1 (**3Ib**)	158.2
Cyclohexyldiol (**5I**)	7.3
Benzopinacol (**6I**)	19.3

Table A2. ONIOM optimizations of the triplet intermediates inside the rigid crystal lattice (no preoptimization of the crystal cavity)

Inclusion compound	ΔE (Ph–CN–Ph), kcal mol^{-1}	Method
Toda–Seebach 1:1	−5.7	ONIOM/Dreiding
	−2.9	ONIOM/MM3
	−3.9	MM3
	1.5	ROHF/6-31G*, biradical
	−1.4	ONIOM(6-31G*)/MM3
Toda–Seebach 2:1	14.7	ONIOM/Dreiding
	8.2	ONIOM/MM3
	4.1	MM3
	5.8	ROHF/6-31G*, biradical
	7.0	ONIOM(6-31G*)/MM3
Cyclohexyldiol	28.6	ONIOM/Dreiding
	16.5	ONIOM/MM3
	12.8	MM3
	7.7	ROHF/6-31G*, biradical
	14.7	ONIOM(6-31G*)/MM3
Benzopinacol	22.5	ONIOM/Dreiding
	37.5	ONIOM/MM3
	33.9	MM3
	7.8	ROHF/6-31G*, biradical
	35.8	ONIOM(6-31G*)/MM3

A sequence of steps necessary to study theoretical aspects of solid-state photochemistry

1. Solving X-ray structure.
2. Using 'Smartpack' or 'Icpack' (for inclusion compounds) to generate the minicrystal lattice.
3. Superposition of the 'ab initio optimized' intermediates on central molecule of the minicrystal lattice.
4. Choosing optimized (inner) and frozen (outer) shells.
5. Preoptimization of the inner shell (reaction cavity) and the intermediate by MM3 inside the frozen outer shell.
6. Cutting the preoptimized reaction cavity (the inner shell) and the intermediate out of the large minicrystal lattice.
7. Optimization of the triplet intermediates (high level, ROHF) inside the frozen preoptimized reaction cavity (low level, Dreiding) using two-level ONIOM calculations as incorporated in GAUSSIAN98.
8. Single point calculations substituting Dreiding energies to MM3 and ROHF(3-21G) energies to ROHF(6-31G*).
9. Recalculating the ONIOM energies.

References

1. This is Paper 188 of our photochemical series and Paper 254 of our general series.
2. For Paper 252 see Zimmerman, H. E.; Ignatchenko, A. *J. Org. Chem.* **1999**, *64*, 6635–6645. For Paper 253 see below, Ref. 10.
3. (a) Zimmerman, H. E.; Zuraw, M. J. *J. Am. Chem. Soc.* **1989**, *111*, 2358–2361. (b) Zimmerman, H. E.; Zuraw, M. J. *J. Am. Chem. Soc.* **1989**, *111*, 7974–7989.
4. (a) Zimmerman, H. E.; Zhu, Z. *J. Am. Chem. Soc.* **1994**, *116*, 9757–9758. (b) Zimmerman, H. E.; Zhu, Z. *J. Am. Chem. Soc.* **1995**, *117*, 5245–5262.
5. Zimmerman, H. E.; Sebek, P. *J. Am. Chem. Soc.* **1997**, *119*, 3677–3690.
6. Zimmerman, H. E.; Sebek, P.; Zhu, Z. *J. Am. Chem. Soc.* **1998**, *120*, 8549–8550.
7. With regard to this approach, one referee's comment was that lattice constraints, possibly 50 Å distant, may play a role not included in the inert gas model.
8. (a) Maseras, F.; Morokuma, K. *J. Comp. Chem.* **1995** *16*, 1170–1179. (b) Matsubara, T.; Sieber. S.; Morokuma, K. *Int. J. Quantum Chem.*, **1996**, *60*, 1101–1109. (c) Frisch, M. J.; Trucks, G. W.; Schlegel, H. B.; Scuseria, G. E.; Robb, M. A.; Cheeseman, J. R.; Zakrzewski, V. G.; Montgomery, Jr., J. A.; Stratmann, R. E.; Burant, J. C.; Millam, J. M.; Daniels, A. D.; Kudin, K. N.; Strain, M. C.; Farkas, O.; Tomasi, J.; Barone, V.; Cossi, M.; Cammi, R.; Mennucci, B.; Pomelli, C.; Adamo, C.; Clifford, C.; Ochterski, J.; Petersson, G. A.; Ayala, P. Y.; Cui, Q. K.; Morokuma, K.; Malick, D. K.; Rabuck, A. D.; Raghavachari, K.; Foresman, J. B.; Cioslowski, J.; Ortiz, J. V.; Stefanov, B. B.; Liu, G.; Liashenko, A.; Piskorz, P.; Komaromi, I.; Gomperts, R.; Martin, R. L.; Fox, D. J.; Keith, T.; Al-Laham, M. A.; Peng, C. Y.; Nanayakkara, A.; Gonzalez, C.; Challacombe, M.; Gill, P. M. W.; Johnson, B.; Chen, W.; Wong, M. W.; Andres, J. L.; Gonzalez, C.; Head-Gordon, M.; Replogle, E. S.; Pople, J. A. GAUSSIAN 98, Revision A.6, Gaussian, Inc., Pittsburgh PA, 1998. (d) The literature has a number of QM/MM programs described but mainly dealing with solvation and similar aspects.

9. Zimmerman, H. E.; Rieke, R. D.; Scheffer, J. R. *J. Am. Chem. Soc.* **1967**, *89*, 2033–2047.
10. Zimmerman, H. E.; Alabugin, I. V.; Chen, W.; Zhu, Z. *J. Am. Chem. Soc.* **1999**, *121*, 11930–11931.
11. (a) Beck, A. K.; Bastani, B.; Plattner, D. A.; Petter, W.; Seebach, D.; Braunschweiger, H.; Gysi, P.; Vecchia, L. L. *Chimia* **1991**, *45*, 238–244. (b) Seebach, D.; Beck, A. K.; Imwinkelried, R.; Roggo, S.; Wonnacott, A. *Helv. Chim. Acta.* **1987**, *70*, 954–974.(c) Toda, F.; Tanaka, K. *Tetrahedron Lett.* **1988**, *29*, 551–554.
12. Chiral hosts have been used for resolution. See: (a) See Ref. 11b. (b) Toda, F. *Acc. Chem. Res.* **1995**, *28*, 1059–1062; (c) Korkas, P. P.; Weber, E.; Czugler, M.; Naray-Szabo, G. *J. Chem. Soc. Chem. Commun.* **1995**, *21*, 2229–2230.
13. We thank Dr Douglas J. Fox of Gaussian, Inc. for informal advice on the use of Oniom.
14. Mayo, S. L.; Olafson, B. D.; Goddard, W. A. *J. Phys. Chem.* **1990**, *94*, 8897–8909.
15. Rappe, A. K.; Casewit, C. J.; Colwell, K. S.; Goddard, W. A.; Skiff, W. M. *J. Am. Chem. Soc.* **1992**, *114*, 10024–10035.
16. Allinger, N. L. *MM3*, University of Georgia, December 1990.
17. (a) This convenient notation was introduced along with theory correlating photochemical reactivity to excited state electronic structure. The notation permits thinking in three dimensions while writing in two. (b) Zimmerman, H. E. *Abstracts of the Seventeenth National Organic Symposium of the American Chemical Society*, Bloomington, Indiana, 1961; pp 31–41. (b) Zimmerman, H. E.; Schuster, D. I. *J. Am. Chem. Soc.* **1962**, *84*, 4527–4540. (c) Zimmerman, H. E.; Noyes, Jr., Hammond, A G. S., Pitts, Jr., J. N., Eds.; *Advances in Photochemistry*; Interscience: New York, 1963, Vol. 1, pp 183–208.
18. Zimmerman, H. E.; Lewin, N. *J. Am. Chem. Soc.* **1969**, *91*, 879–886.
19. Mohamadi, F.; Richards, N. G. J.; Guida, W. C.; Liscamp, R.; Lipton, M.; Caufield, C.; Chang, G.; Hendrickson, T.; Still, W. C. MacroModel V6.5. *J. Comput. Chem.* **1990**, *11*, 440.
20. (a) McBride, J. M. *Acc. Chem. Res.* **1983**, *16*, 304–312; (b) Kearsley, S. K.; McBride, J. M. *Mol. Liq. Cryst. Inc. Nonlin. Opt.* **1988**, *156* 109–122.
21. (a) Gavezzotti, A.; Simonetta, M. *Chem. Rev.* **1982**, *82*, 1–13. (b) Peachey, N. M.; Eckhardt, C. J. *J. Phys. Chem.* **1994**, *98*, 7106–7115; (c) Leibovitch, M.; Olovsson, G.; Sundarababu, G.; Ramamurthy, V.; Scheffer, J. R.; Trotter, J. *J. Am. Chem. Soc.* **1996**, *118*, 1219–1220; (d) Ariel. S.; Askarai, S.; Scheffer, J. R.; Trotter, J.; Walsh, L. *J. Am. Chem. Soc.* **1984**, *106* 5726–5728. (e) Ramamurthy, V.; Venkatesan, K. *Chem. Rev.* **1987**, *87*, 433–481; (f) Ito, Y. *Synthesis*, **1998**, 1–32. (g) Shin, S. H.; Huang, F. K.; Garcia-Garibay, M. *Tetrahedron Lett.* **1999**, 261–264. (h) Keating, A. E.; Shin, S. H.; Houk, K.; Garcia-Garibay, M. *J. Am. Chem. Soc.* **1997**, *119*, 1474–1475; (i) Leibovitch, M.; Olovsson, G.; Scheffer, J. R.; Trotter, J. *J. Am. Chem. Soc.* **1998**, *120*, 12550–12551; (j) Singh, N. B.; Singh, R. J.; Singh, N. P. *Tetrahedron* **1994**, *50*, 6441–6493.
22. Sheldrick. G. M. SHELXTL Version 5 Reference Manual. Siemens Analytical X-ray Instruments, 6300 Enterprise Dr., Madison, WI 53719-1173, USA, 1994.